

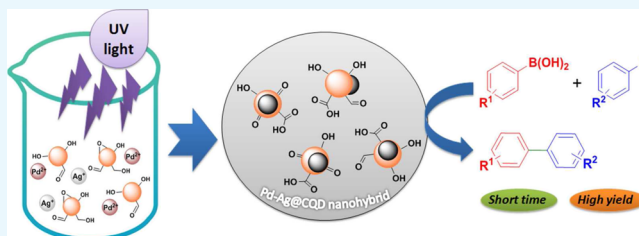
Photo-Assisted Synthesis of a Pd–Ag@CQD Nanohybrid and Its Catalytic Efficiency in Promoting the Suzuki–Miyaura Cross-Coupling Reaction under Ligand-Free and Ambient Conditions

Rajarshi Bayan and Niranjan Karak*[✉]

Advanced Polymer and Nanomaterial Laboratory, Department of Chemical Sciences, Tezpur University, Napaam, 784028 Tezpur, Assam, India

S Supporting Information

ABSTRACT: Supported bimetallic nanoparticles are very promising heterogeneous catalysts for carbon–carbon cross-coupling reactions, though reports focusing on their synergistic activity for promoting such reactions are very limited. In the current study, bimetallic Pd–Ag hybrid nanoparticles supported on carbon quantum dots (CQDs), Pd–Ag@CQDs, were synthesized by a facile and fast UV-light-driven (365 nm) one-pot protocol for the first time to investigate such a synergistic activity. The physico-chemical structural features of the Pd–Ag@CQD nanohybrid were evaluated by UV–vis, Fourier transform infrared, X-ray diffraction, electron-dispersive X-ray, and transmission electron microscopy analyses. The nanohybrid was found to have dimensions in the range of ca. 3–5 nm. The bimetallic Pd–Ag@CQD nanohybrid was utilized as an efficient heterogeneous catalyst for promoting the Suzuki–Miyaura coupling reaction with aryl bromides and aryl chlorides under ligand-free and ambient conditions. The synergistic activity of the components of the nanohybrid induced catalytic enhancement of the cross-coupling reaction in terms of short reaction times (<1 h) and high yields (>90%). The heterogeneous character of the nanohybrid system also enabled easy separation and recyclability (up to six cycles).



INTRODUCTION

Carbon–carbon (C–C) cross-couplings are one of the most relevant research topics in the current synthetic chemistry. These coupling reactions provide a significant tool for the construction of many important compounds.¹ In this context, the pioneering efforts of Suzuki, Heck, and Negishi toward palladium-catalyzed C–C cross-coupling reactions are the benchmark for modern synthetic organic chemistry.² The Suzuki–Miyaura cross-coupling reaction is arguably one of the most widely applied C–C bond formation reactions till date. The aforementioned reaction provides a potent synthetic pathway for preparing biaryl compounds, which are generally used in fields of natural products, pharmaceuticals, agro-chemicals, and polymers.³ The traditional Suzuki–Miyaura cross-coupling reaction utilizes homogeneous palladium complexes with ligands (such as phosphine) as catalysts.⁴ Despite high activity and selectivity of these catalytic systems, challenges associated with their recovery and recyclability limit their utility in the industrial process. Further, challenges in preparation, cost, and use of toxic ligands (e.g., phosphine) confine the aptness of such catalysts in large-scale applications.⁵ In this milieu, heterogeneous palladium catalysts presents a promising avenue to address these setbacks as validated by the continuing research efforts in this area.⁶

Again in recent times, nanocatalysis is being widely applied in promoting synthetic organic transformations. These catalysts generally consist of nano-dimensional active components (metal/metal oxides) dispersed over a solid support. The

catalytic activity, selectivity, and stability of these nanocatalysts mainly depend upon their shape, size, composition, and structure.⁷ These nano-dimensional particles enhance the surface area of the catalyst, thereby increasing the chances of contact between the reactants and the catalyst. Moreover, their heterogeneous nature makes them easily separable from the reaction mixture, thereby facilitating easy product isolation. In this regard, palladium-based nanocatalysts are emerging as one of the most exciting alternative catalysts in the field of C–C cross-coupling reactions owing to their high activity and selectivity compared to conventional catalysts.⁸ As a matter of fact, recent reports on Pd nanoparticle-catalyzed C–C cross-couplings still suggest its crucial importance in this scenario.⁹ Furthermore, considerable efforts are being devoted to immobilization and stabilization of Pd nanoparticles (PdNPs) in various heterogeneous supports such as organic matrices, organic–inorganic fluorinated hybrid materials, polymers, glass–polymer composites, ionic liquids, and so forth. In addition, PdNPs are also being synthesized with organic–inorganic supports such as carbon,¹⁰ carbon nanotubes,¹¹ graphene,¹² alumina,¹³ silica,¹⁴ zeolite,¹⁵ clays,¹⁶ iron oxide,¹⁷ and zinc ferrite¹⁸ for promoting C–C couplings. More recently, biosynthesized PdNPs are also reported for showing promising catalytic action toward C–C

Received: October 7, 2017

Accepted: November 28, 2017

Published: December 12, 2017

cross-coupling.¹⁹ However, major drawbacks of such nanocatalysts include aggregation of PdNPs and the need for additives and stabilizers that hamper the overall reaction process.

In this juncture, carbon quantum dots (CQDs) represent an interesting choice of support because of its high surface functionality, chemical stability in various media, and inertness to supported metals. CQDs are promising class of carbon nanomaterials composed of amorphous and poor crystalline carbon cores (predominantly graphitic sp^2 domains) with sizes varying from 2 to 10 nm.²⁰ Apart from displaying a fascinating size- and excitation wavelength-dependent photoluminescence behavior, CQDs show unique properties such as excellent aqueous solubility at the nano level, high photostability, and biocompatibility. All of these factors allow CQDs to be considered as green, benign, and inexpensive nanomaterials with a wide range of applicability.²¹ In addition, their facile mass scale production from bioresources promotes their variety of applications. However, the potential of CQDs remains barely explored in terms of catalytic applications in synthetic organic chemistry, as compared to other carbon-based nanomaterials such as carbon nanotubes and graphene. In this regard, our group is currently engaged in exploring the photo-catalytic activity of CQDs with the emphasis on promoting clean and green synthetic transformations.²² However, surprisingly, only a few literature reports cite the use of CQDs in C–C cross-coupling reactions, with very little information on their role.²³ Keeping this in mind, CQDs are used as sites of nucleation and growth of NPs, forming new functional materials in turn, where CQDs may play a pivotal role in stabilization of the metal NPs and enhancement of catalytic activity. Hence, the utilization of CQDs in the formation and stabilization of Pd–Ag NPs may lead to a stable catalytic system for the Suzuki–Miyaura coupling reaction. Moreover, the heterogeneity of the system can offer advantage in terms of catalyst recovery and recyclability.

Herein, we report the synthesis of a nanohybrid system of Pd–Ag hybrid NPs supported over CQDs by a facile UV-light-driven reduction process using CQDs as the “green” reductant and stabilizer. The synthesized nanohybrid was characterized by using UV–vis, Fourier transform infrared (FT-IR), electron-dispersive X-ray (EDX), and transmission electron microscopy (TEM) analyses. The Pd–Ag@CQD nanohybrid was employed as the heterogeneous catalyst for promoting the Suzuki–Miyaura cross-coupling reactions of aryl boronic acids with aryl bromides and aryl chlorides under ligand-free and ambient conditions. The nanohybrid was found to immensely enhance the reaction rate and the product yield. This catalytic enhancement of the reaction was investigated using different variants of the components of the nanohybrid.

■ INSTRUMENTATION

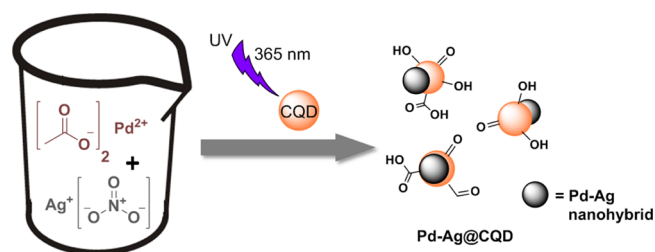
UV–visible spectra were observed by a UV–visible spectrophotometer (model: UV-300, Thermo Fisher, USA). FT-IR spectra were recorded on an FT-IR spectrophotometer (model: Impact 410, Nicolet, USA) using KBr pellets. The X-ray diffraction (XRD) patterns were measured with the help of a powdered XRD (PXRD) machine (model: D8 FOCUS, Bruker AXS, Germany) operating at a wavelength of 1.5 Å and Cu $K\alpha$ as a irradiation source. The size, shape, and distribution of the nanohybrid were observed from a transmission electron microscope (model: JEM-2100, JEOL, Japan) at an operating voltage of 200 kV using Cu grid Ultrathin C, Type A, 400 mesh. The microscopic data were analyzed for inverse fast Fourier transform (IFFT) images by using Gatan DigitalMicrograph

software. The elemental composition of the nanohybrid was confirmed through an EDX technique using a scanning electron microscopy (SEM) (model: JSM 6390LV, JEOL, Japan) instrument. The surface area of the nanohybrid was analyzed by Brunauer–Emmett–Teller (BET) analysis (model: 1000E, Quantachrome, USA). The analysis of leaching of elements was done by inductively coupled plasma mass spectrometry (ICP-MS, model: NexION 2000, PerkinElmer, USA). The characterization of the isolated products was carried out using ^1H and ^{13}C NMR on an NMR instrument (model: ECS-400, JEOL, Japan) using tetramethylsilane as the internal standard and CDCl_3 as the solvent.

■ RESULTS AND DISCUSSION

Synthesis and Characterization of the Pd–Ag@CQD Nanohybrid. The bimetallic Pd–Ag@CQD nanohybrid was synthesized by in situ reduction of Pd^{2+} and Ag^+ ions with as-prepared CQDs through a UV irradiation-assisted one-step wet chemical protocol, as depicted in Scheme 1.

Scheme 1. Synthesis of the Pd–Ag@CQD Nanohybrid



It is widely reported that CQDs are capable of reducing metal salts.^{23,25} In the current process, CQDs acted as both reducing as well as stabilizing agents. As reported earlier, the surfaces of CQDs are enriched with diverse polar functionalities such as alkoxyl, hydroxyl, epoxy, aldehydic carbonyl, and carboxylic groups.²¹ These surface functionalities facilitated the complexation of Pd^{2+} and Ag^+ ions with CQDs and subsequently helped in their reduction to Pd^0 and Ag^0 . In addition, CQDs promoted nucleation-oriented growth of these NPs on their surfaces and helped in their stabilization. The reduction process was greatly augmented by the excellent electron-releasing ability of photo-excited CQDs under UV radiation ($\lambda_{\text{exc}} = 365 \text{ nm}$), leading to a dramatic decrease in the reduction time. It is demonstrated earlier that photo-excited CQDs can serve as both electron donors and electron acceptors, owing to their photo-ripening capability.^{22,26} Further evidence for the reduction of Pd^{2+} and Ag^+ ions by CQDs was obtained by observing the dramatic quenching of the signatory fluorescence emissions of CQDs (Figure S1 of the Supporting Information). This UV-light-assisted fast reduction process was validated by control experiments conducted under dark and visible light, both of which were recorded for longer durations (Table S1 of the Supporting Information). Various literature suggested the role of peripheral polar moieties, especially hydroxyl groups and aldehydic groups, in the reduction of metal ions.²⁷ In this study, presumably aldehydic, alkoxyl, epoxy, and hydroxyl groups of CQDs played a pivotal role in simultaneous reduction of both Pd^{2+} and Ag^+ ions. Details of the reduction mechanism and formation of the nanohybrid have been provided in Scheme 2.

A UV–vis study suggested the formation of the Pd–Ag@CQD nanohybrid, considering the changes in absorbance from

Scheme 2. Mechanism of UV-Light-Assisted Reduction and Subsequent Formation of the Pd–Ag@CQD Nanohybrid

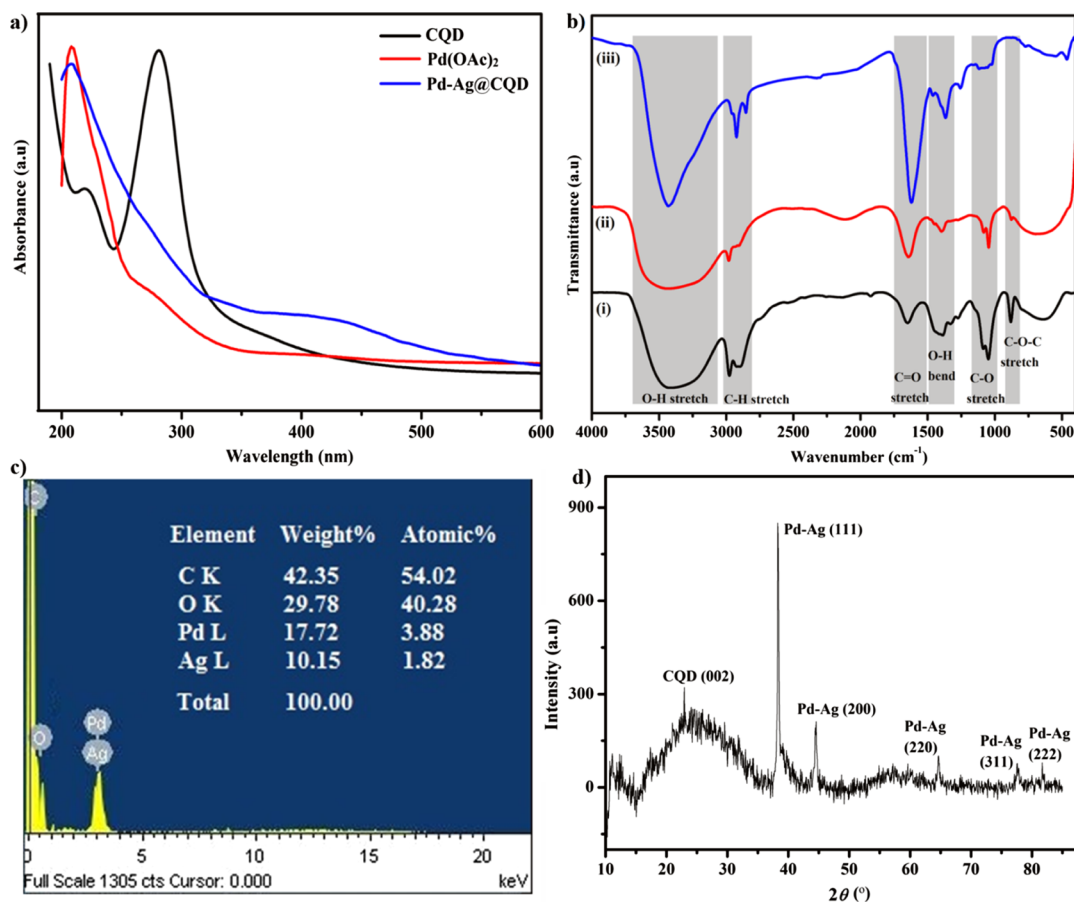
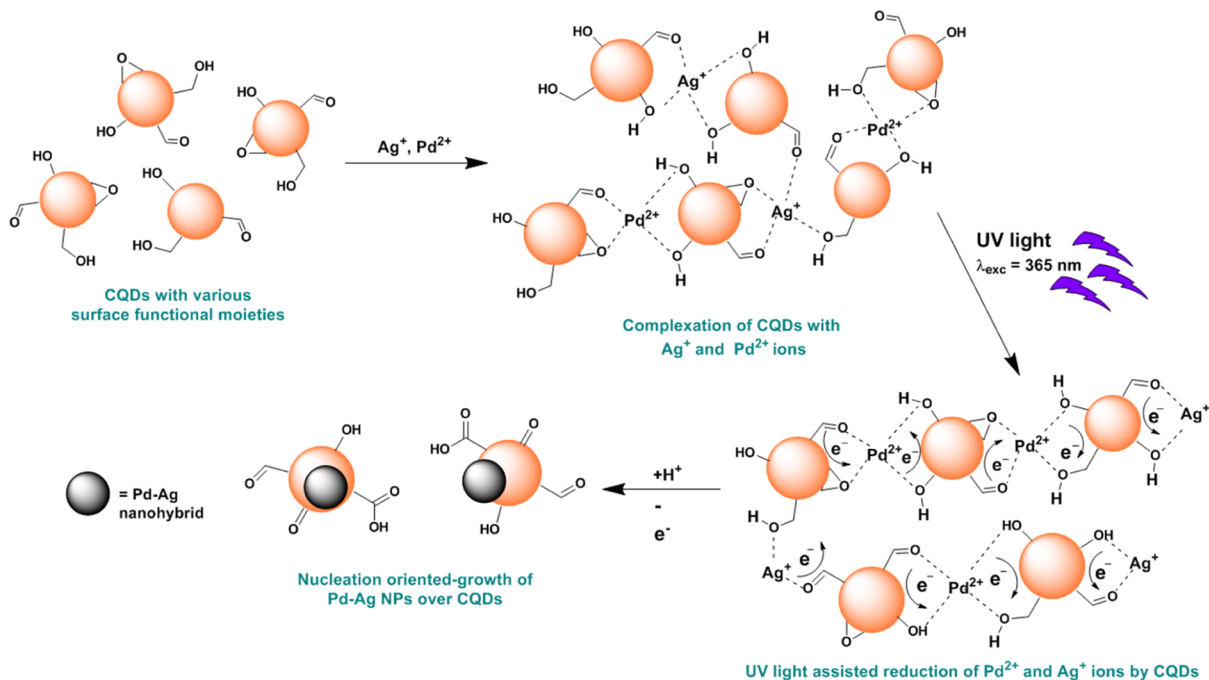


Figure 1. (a) UV spectra of CQD, Pd(OAc)₂, and the Pd–Ag@CQD nanohybrid; (b) FT-IR spectra of (i) CQD, (ii) Pd²⁺–Ag⁺–CQD complex, and (iii) Pd–Ag@CQD nanohybrid; (c) EDX map of the Pd–Ag@CQD nanohybrid; and (d) PXRD patterns of the Pd–Ag@CQD nanohybrid.

its precursors (Figure 1a). The characteristic absorbance peaks of CQDs at 220 and 280 nm were either obscured or diminished, along with the absorbance peak of the Pd²⁺ ion at 282 nm.^{19a,24}

Further, the appearance of a continuous absorbance with a weak shoulder between 300 and 380 nm was attributed to PdNPs, followed by a broad peak at 420 nm corresponding to surface

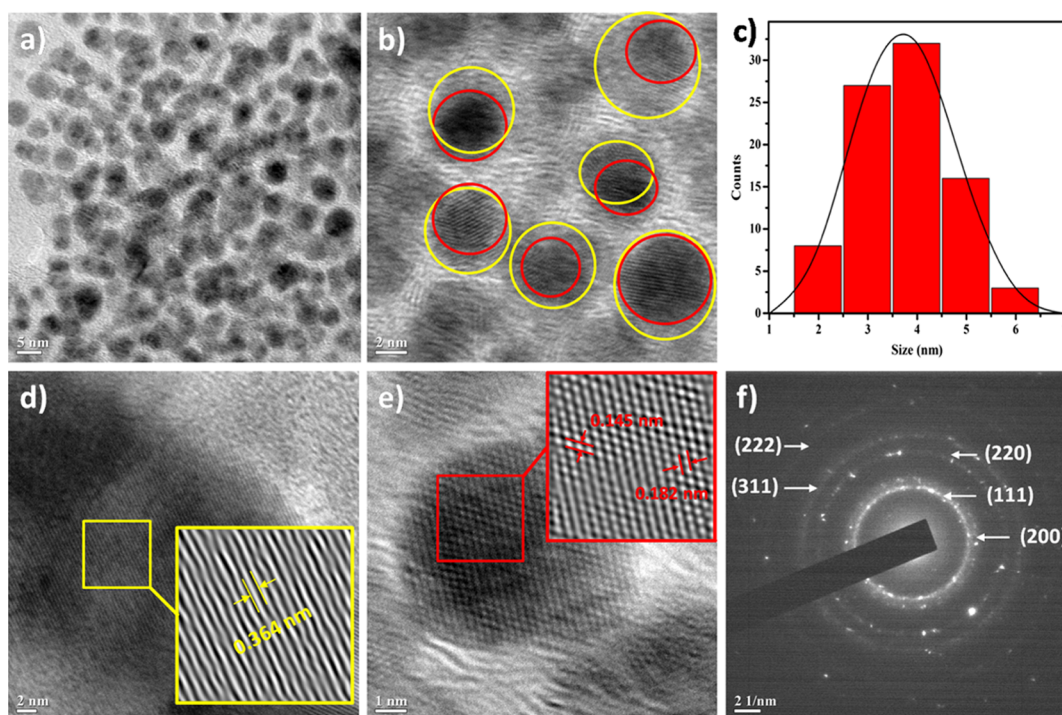


Figure 2. (a,b) TEM images of Pd–Ag@CQD; (c) size distribution of Pd–Ag@CQDs; (d) HRTEM of the CQD phase; (e) HRTEM of the Pd–Ag nano hybrid phase; and (f) SAED pattern of Pd–Ag@CQDs.

plasmon resonance of Ag nanoparticles (AgNPs) pointed toward the presence of the bimetallic Pd–Ag hybrid phase. Such strong but broad surface plasmon peaks are well-known in the case of various metal NPs. The absorbance appears over the wide range of 200–1200 nm.²⁸ These results strongly indicated the role of CQDs as the reducing agent in the formation of the nano hybrid and supported the proposed reduction and formation mechanism involving nucleation and formation of the Pd–Ag nano hybrid on the surface of CQDs.

FT-IR analysis further revealed key changes in the surface functionalities of CQDs before (i), during (ii), and after (iii) the formation of the Pd–Ag@CQD nano hybrid (Figure 1b). The broad O–H stretching band of CQD, because of extensive H-bonding between the hydroxyl moieties, underwent further broadening during the complexation with Pd²⁺ and Ag⁺. Ultimately, this broad O–H band underwent sharpening at 3400 cm⁻¹ after the formation of the nano hybrid, which indicated the strengthening of the hydroxyl functional groups, possibly stabilizing the Pd–Ag hybrid particles. The C–H stretching bands underwent a similar transition during the process, before finally sharpening at 2926 and 2853 cm⁻¹ after the formation of the nano hybrid. Similarly, the C=O (carbonyl) stretching band of CQDs endured intensification during the complexation, along with more intensification and minute shifting from 1650 to 1670 cm⁻¹ after the formation of the nano hybrid. This plausibly indicated the oxidation of alkoxy and hydroxyl groups to carbonyl groups on reduction of Pd²⁺ and Ag⁺. The change in the O–H bending band of CQDs after the formation of the nano hybrid seen at 1360 cm⁻¹ further demonstrated the change in hydroxyl functional groups because of the presence of the Pd–Ag hybrid particles. Further, the sharp C–O (alkoxy) stretching band at 1044 cm⁻¹ and the oxirane C–O–C stretching band at 886 cm⁻¹ of CQDs diminished in due course of complexation and formation of the nano hybrid, undergoing transformation to C=O groups as described before.

These changes in the intensity and shifting of the band positions in the nano hybrid clearly indicated the strong interactions between CQDs and the bimetallic Pd–Ag hybrid phase. Similar observations were reported by Dey et al.^{23a} and Shen et al.²⁵ These prominent observations pointed toward the contribution of alkoxy, carbonyl, oxirane, and hydroxyl groups in the nano hybrid formation and thereby provided ample evidence in favor of the presumed reduction and nano hybrid formation mechanism.

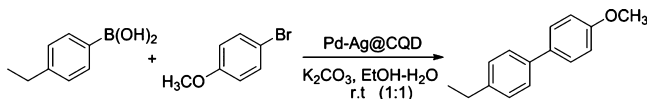
EDX analysis confirmed the presence of elements like C, O, Pd, and Ag in the nano hybrid, with the corresponding wt % values of 42.35, 29.78, 17.72, and 10.15, respectively (Figure 1c). PXRD analysis results gave interesting evidence regarding the physical structure of the nano hybrid (Figure 1d). The nano hybrid displayed the characteristic broad peak of CQDs centered at $2\theta = 23^\circ$ (d -spacing of 3.7 Å), indicating the presence of CQDs. Moreover, the nano hybrid exhibited five sharp diffractions indexed as (111), (200), (220), (311), and (222) planes of a face-centered-cubic (fcc) lattice with corresponding peaks at $2\theta = 38.2^\circ$ (d -spacing of 2.29 Å), 44.5° (d -spacing of 1.98 Å), 64.6° (d -spacing of 1.40 Å), 77.5° (d -spacing of 1.19 Å), and 81.8° (d -spacing of 1.14 Å), respectively. PdNPs and AgNPs are known to exhibit the typical fcc lattice of Pd and Ag metals.^{12a} Surprisingly, no characteristic diffraction peaks for pure Pd or Ag were observed for the nano hybrid. This phenomenon suggested that Ag entered into the Pd crystal lattice, merging together to form a single crystalline Pd–Ag hybrid phase possibly during nucleation-oriented growth over CQDs.^{12b,29} BET analysis revealed that the N₂ adsorption–desorption isotherm of the prepared catalyst shows a type V isotherm and the surface area of the nano hybrid to be 674.327 m² g⁻¹ (Figure S2 of the Supporting Information).

Morphological characteristics of the nano hybrid including shape, size, and particle distribution envisioned by TEM analysis and confirmed the presence of the Pd–Ag nano hybrid particles

supported over CQDs. TEM images displayed near-spherical morphology and uniform particle distribution of the nanohybrid, albeit with some amount of agglomeration (Figure 2a). The Pd–Ag nanohybrid particles (in red circles) nucleated upon CQDs (in yellow circles), thereby forming a stable and supportive nanohybrid system (Figure 2b). Statistical analysis revealed that the size distribution lies between 2 and 6 nm, and the largest fraction of particles possessed sizes in the range of 3–5 nm (Figure 2c). High-resolution TEM (HRTEM) images of Pd–Ag@CQD further showed the presence of lattice fringes (Figure 2d,e). Conversion of selected areas (in yellow and red squares) into corresponding IFFT images revealed different interplanar distances (inset). The interplanar distance of 0.364 nm was attributed to lattice planes of CQDs, which is close to the (002) crystallographic plane of CQDs, whereas the interplanar distances of 0.185 and 0.145 nm were attributed to lattice planes of the Pd–Ag nanohybrid phase, which is close to (200) and (220) planes of the Pd–Ag hybrid.^{12a} Selected area diffraction (SAED) patterns of the nanohybrid are in good agreement with the crystalline Pd–Ag nanohybrid phase, which were also consistent with PXRD pattern results.

Catalytic Application of the Pd–Ag@CQD Nanohybrid in Suzuki–Miyaura Cross-Coupling Reaction. The catalytic activity of the Pd–Ag@CQD nanohybrid was evaluated in the Suzuki–Miyaura cross-coupling reaction. For this purpose, the coupling of 4-ethylphenylboronic acid with 4-bromoanisole was chosen as the model reaction using ethanol–water (1:1) as the solvent system and K₂CO₃ as the base. 1 wt % of the Pd–Ag@CQD nanohybrid, with respect to 4-ethylphenylboronic acid, was employed as the catalyst. The reactions were performed at room temperature under aerobic conditions without the addition of any ligands or additives (Scheme 3). The reaction afforded 4-

Scheme 3. Model Reaction for Pd–Ag@CQD-Catalyzed Suzuki–Miyaura Cross-Coupling



ethyl-4'-methoxy-1,1'-biphenyl with a 70% yield in 4 h. For this reaction, an ethanol–water mixture (1:1) provided a highly polar co-solvent system in which the substrates were easily homogenized, and thus, it acts as a stable dispersion medium for the nanohybrid catalyst. Moreover, the choice of the ethanol–water solvent offered a neat and green reaction medium. In similar lines, the choice of K₂CO₃ presented a mild, inexpensive, effective base necessary for the cross-coupling reaction.

To study the effect of the catalyst loading on the reaction rate and its efficiency, the model reaction was utilized, and the results are summarized in Table 1. From this study, it was observed that the catalyst loading is essential for the reaction to proceed (entry 1). Also, it was seen that the catalyst loading affected the reaction rate, in correlation with the reaction time and the product yield (entry 2–5). Further, it was found that catalytic loading of 5 wt % was the optimized amount for the coupling reaction (entry 4), as a further increase in catalyst loading to 7.5 wt % did not have any substantial increment in the reaction rate and its efficiency (entry 5). Catalytic loading of 10 wt % eventually led to the decrease in the yield, with some amount of agglomeration observed in the reaction medium (entry 6). This may also be caused by

Table 1. Effect of Catalyst Loading on the Suzuki–Miyaura Coupling Reaction^a

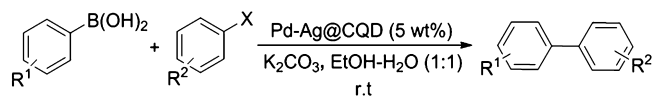
entry	catalyst loading (wt %) ^b	time (h)	yield (%) ^c
1	Nil	12	0
2	1	4	70
3	2.5	3	85
4	5	1	94
5	7.5	1	94
6	10	1	89

^aReaction conditions: 4-ethylphenylboronic acid (0.255 mmol, 0.0379 g), 4-bromoanisole (0.25 mmol, 0.0467 g), K₂CO₃ (1.0 mmol, 0.138 g), and EtOH–H₂O (4 mL). ^bwt % wrt 4-ethylphenylboronic acid. ^cIsolated yield.

adsorption of some amount of reactants on the surface of the catalyst.

To determine the applicability and limitation of the current procedure, reactions of different aryl boronic acid derivatives with substituted/unsubstituted aryl bromides and aryl chlorides were examined using the optimized conditions. Aryl bromides/chlorides were chosen for this purpose as the activation of C–Br or C–Cl bonds are tougher than C–I bonds.² The results are summarized in Table 2.

Table 2. Substrate Study for the Pd–Ag@CQD-Catalyzed Suzuki–Miyaura Coupling Reaction^{a,b,c}



entry	R ¹	R ²	X	time (h)	yield (%)
1	H	H	4-Br	1	97
2	H	4-OCH ₃	4-Br	1	94
3	H	4-NO ₂	4-Br	1.2	90
4	CH ₂ CH ₃	H	4-Br	1	92
5	CH ₂ CH ₃	4-OCH ₃	4-Br	1	94
6	3-NO ₂	H	4-Br	1.4	90
7	3-CF ₃	4-OCH ₃	4-Br	1.8	83
8	3-NO ₂	4-NO ₂	4-Br	3	74
9	2-naphthyl	4-OCH ₃	4-Br	1	92
10	4-OCH ₃	4-OH	4-Br	1	90
11	H	H	4-Cl	24	25
12	CH ₂ CH ₃	H	4-Cl	16	30

^aReaction conditions: aryl boronic acid (0.255 mmol), aryl halide (0.25 mmol), K₂CO₃ (1.0 mmol, 0.138 g), and EtOH–H₂O (4 mL). ^bwt % wrt aryl boronic acid. ^cIsolated yield, purified by column chromatography and authenticated by NMR analyses (Fig S4–S15 in the Supporting Information).

From the substrate study, it was observed that rate of the Suzuki–Miyaura cross-coupling reaction depends on the nature of substituents on both the aryl halides and aryl boronic acids. The presence of electron-releasing substituents on the aryl boronic acid as well as on aryl halides required less time to complete, whereas those with electron-withdrawing substituents took a little longer duration for completion. This may be due to the presence of polar electron-releasing moieties on the surface of the nanohybrid catalyst (from CQDs), which facilitated better interactions with the substrates having electron-releasing groups than those with electron-withdrawing groups. Dey et al.^{23a} and Borah et al.^{19a} reported comparable observations regarding the

effect of substituents. In most of the cases, the homo-coupling product was not observed and did not exceed 3% in some cases.

The reusability of the catalyst is very important from the perspective of green and sustainable chemistry. Accordingly, the catalyst was screened for reusability by employing the model reaction for consecutive runs and analyzed by gas chromatography (Figure 3, Table S2 of the Supporting Information). The

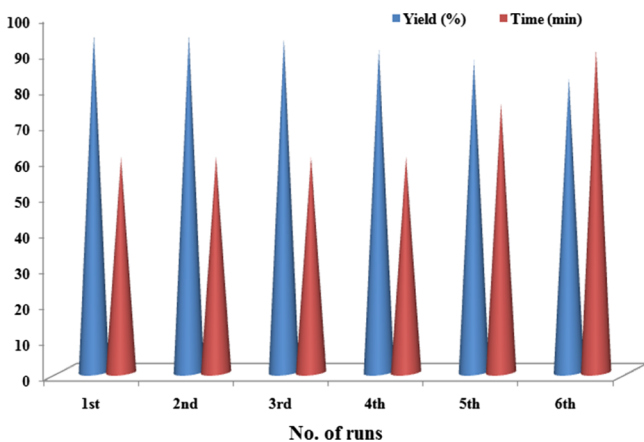


Figure 3. Catalyst reusability in terms of yield and time.

procedure afforded completion of the reaction in the comparable reaction time and the product yield during the first three runs, as that for the fresh catalyst. The catalyst was found to be reusable up to the third run without any loss of the catalytic activity. However, the catalyst demonstrated some amount of agglomeration in the reaction medium after the fourth run, with a slight loss in catalytic activity as manifested by a decrease in the product yield. This slight loss of activity can be attributed to the agglomeration of the nanohybrid, leading to deactivation of the catalytic system after several runs of the reaction and the recovery process. Similar observations were made by Dey et al.,^{23a} Borah et al.,^{19a} and Moussa et al.^{12a} regarding agglomeration of NPs in the reaction medium on subsequent catalytic cycles. To verify any change in the structure and morphology after undergoing several runs, the recovered catalyst was analyzed by PXRD. The results, in general, hinted toward an intact state and the structure of the catalyst, without much significant changes, which are supported by the appearance of previously observed diffraction patterns for the Pd–Ag@CQD nanohybrid (Figure 4a). Also,

the EDX study of the recovered catalyst displayed almost the same elemental composition as seen before (Figure 4b). In addition, the leaching of Pd and Ag in the reaction medium was studied by ICP analysis (Table S3 of the Supporting Information). The study disclosed the leakage of 0.871 ppm Pd and 0.520 ppm Ag in the reaction mixture, amounting to a loss of 0.058% Pd and 0.034% Ag from the total amount of the catalyst. These results suggested the presence of trace amounts of Pd and Ag soluble in the reaction medium; however, because the amount was less than 1 ppm, the leakage can be treated as very minute.

The highest turnover number (TON) and turnover frequency (TOF) were found to be 752.3 and 12.53 min⁻¹, respectively, for Pd–Ag@CQDs for the cross-coupling reaction. Details on calculation of TON and TOF are provided in the Supporting Information.

The mechanism of the C–C cross coupling reactions catalyzed by heterogeneous palladium catalysts is a subject of great scientific interest, as to identify the exact species responsible for the catalysis.³ However, it is widely accepted that the mechanism follows a heterogeneous catalytic cycle. The heterogeneity of the catalyst was supported by using the hot filtration test, as discussed in the Supporting Information, Figure S3; however, there was a very miniature amount of leached metals in the filtrate as detected by ICP analysis.

Study of the Catalytic Role of the Components of the Pd–Ag@CQD Nanohybrid in the Suzuki–Miyaura Cross-Coupling Reaction. From the catalyst optimization study and substrate study, it was seen that the Suzuki–Miyaura cross-coupling reaction was greatly enhanced by the Pd–Ag@CQD nanohybrid in terms of the reaction time and yield. To explain the basis of this enhancement, that is, the role of the components in the nanohybrid system, the reaction was emulated with different variants of the catalyst viz., CQDs, AgNP, PdNPs, and the results are summarized in the Table 3. For this purpose, the Suzuki–Miyaura cross-coupling reaction of the aryl boronic acid derivative and aryl chloride was chosen to be the model reaction. This is because, as the reaction with aryl bromides was comparatively faster and easier, the toughest reaction conditions, that is, with aryl chlorides, were emulated for better understanding of the role of the catalyst in the cross-coupling reaction.

From the study, it was observed that the reaction did not proceed in the presence of only CQDs as the catalyst (entry 1). A similar observation was made when only AgNPs were used in

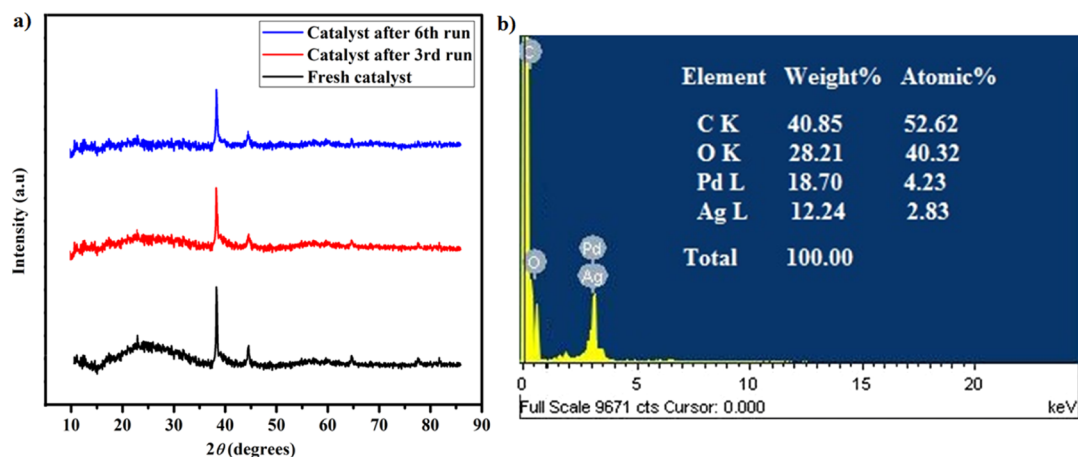
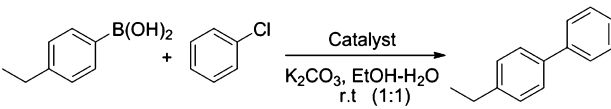


Figure 4. (a) PXRD patterns of the recovered catalyst and (b) EDX map of the recovered catalyst.

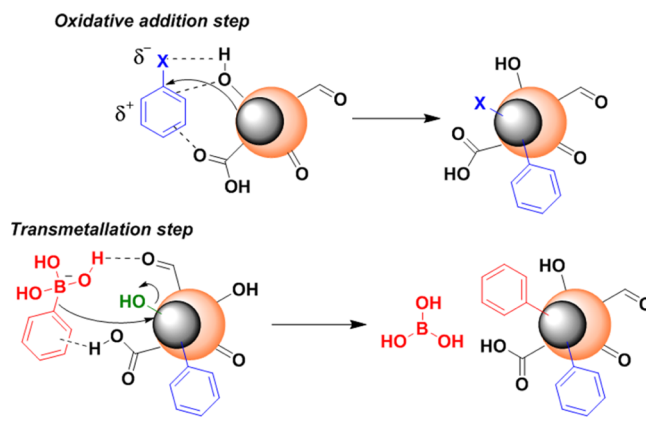
Table 3. Study of the Role of Components of the Nanohybrid for Suzuki–Miyaura Cross-Coupling


entry	catalyst	time (h)	yield (%) ^a
1	CQDs ^d	24	NR
2	AgNPs ^c	24	NR
3	PdNPs ^b	32	16
4	PdNPs ^b + AgNPs ^c	32	22
5	AgNPs ^c + CQDs ^d	24	NR
6	PdNPs ^b + CQDs ^d	24	20
7	PdNPs ^b + AgNPs ^c + CQDs ^d	22	25
8	Pd–Ag@CQD ^b	16	30

^aIsolated yield. ^b5 wt % wrt phenyl boronic acid derivative. ^c5 wt % wrt phenyl boronic acid derivative. ^d2 wt % wrt phenyl boronic acid derivative.

catalytic amounts (entry 2). Both of these initial observations can be attributed to the inability of CQDs and AgNPs to singlehandedly catalyze the reaction. On the other hand, when only PdNPs were used, the reaction proceeded sluggishly, with a very low yield of 16% (entry 3). This can be accredited to the difficulty in activation of the C–Cl bond of aryl chloride under the current reaction conditions. Hence, this outcome necessitates the presence of palladium for the reaction to proceed. Again, when both PdNPs and AgNPs were used in tandem, a slightly better yield of 22% was recorded (entry 4). This pointed toward the role of AgNPs in assisting PdNPs for catalyzing the reaction and signified the catalytic enhancement brought about by the combination of the two. The reaction was not successful with combination of AgNPs and CQDs (entry 5), as observed earlier. However, the combination of PdNPs and CQDs afforded better results with a reduced reaction time and an increased yield of 20% (entry 6). Hence, the presence of CQDs in tandem with PdNPs resulted in the catalytic enhancement of the reaction too. Now, when PdNPs, AgNPs, and CQDs were used together, the reaction time decreased further, and the yield of 25% was recorded (entry 7). The outcome suggested the synergistic ability of CQDs and AgNPs in assisting PdNPs in the catalytic enhancement of the cross-coupling reaction. This result was comparable to the Pd–Ag@CQD nanohybrid system, which recorded the minimum time with a maximum yield (entry 8).

Hence, it can be suggested that Ag and CQDs played a pivotal role in the stabilization and activation of Pd in the nanohybrid, thereby providing crucial assistance during the catalytic process. The integration of Pd with Ag in the nanohybrid augmented the activity of Pd by virtue of synergistic metal–metal interactions, thereby making an energetic electron transfer process feasible between them.³⁰ Additionally, CQDs with their surface functional moieties served as the reaction surface by means of secondary interactions like π – π interactions, H-bonding, and so forth, with the reactants, especially during the oxidative addition and transmetalation steps (Scheme 4). The rate-determining step in the Suzuki–Miyaura cross-coupling reaction, the oxidative addition step, may be accelerated by the activated Pd species, leading to the enrichment of inherent catalytic activity of the reaction. Furthermore, the energy released during electron transfer to the surrounding environment probably contributed to the enhancement of catalytic activity.³⁰

Scheme 4. Synergistic Role of the Pd–Ag@CQD Nanohybrid in the Suzuki–Miyaura Cross-Coupling Reaction

Thus, overall, these observations clearly exhibited that the enhanced activity in the Suzuki–Miyaura cross-coupling reaction might be attributed to the synergistic effect between Pd–Ag hybrid NPs existing adjacent to each other, supported over CQDs.

CONCLUSION

Photo-activated CQDs can be used as the reducing and stabilizing agent for synthesis of the Pd–Ag@CQD nanohybrid by a facile and expeditious single-step protocol. Structural analyses confirmed the formidable structural integration of CQDs with Pd–Ag hybrid NPs in the nanohybrid system. Most interestingly, the Pd–Ag@CQD nanohybrid served as an effective heterogeneous catalyst for the Suzuki–Miyaura cross-coupling reaction under a normal atmosphere and ligand-free conditions. The synergistic action of the components in the nanohybrid induced catalytic enhancement of the cross-coupling reaction in terms of short reaction times and high yields. The heterogeneous nature of the nanohybrid enabled catalyst recovery and reusability.

EXPERIMENTAL SECTION

Materials and Methods. Palladium acetate (Sigma-Aldrich, USA), silver nitrate (Merck, India), and dextrose anhydrous (Merck, India) were utilized as received. CQDs were prepared by microwave irradiation after a slight modification in the reported procedure (as described in the Supporting Information, Scheme S1).²⁴ Other chemicals and solvents were of reagent grade and used without further purification.

Synthesis of the Pd–Ag@CQD Nanohybrid. Pd–Ag@CQDs were synthesized by a facile UV-light-assisted reduction process by employing CQDs as the biobased reducing as well as stabilizing agent. In a typical experiment, 5 mL of 10 mM Pd(OAc)₂ solution and 5 mL of 10 mM AgNO₃ solution in ethanol were taken in a round-bottomed flask. Ten milliliters of as-prepared CQDs (concentration of CQDs was 24 mg/mL) was added to the reaction mixture, and it was stirred under UV light at a wavelength of 365 nm for 1 h. The formation of the Pd–Ag@CQD nanohybrid was indicated by a change in the color of the solution from greenish brown to metallic brown, along with the disappearance of the green luminescence of CQDs with advancing reaction time. The nanohybrid was collected, centrifuged at 5000 rpm, and washed five times with ethanol–water to remove the excess metal salts and unbound CQDs. The obtained nanohybrid was dispersed in ethanol by ultrasonication

and stored under ambient conditions. For structural analysis, the nanohybrid was oven-dried at 45 °C for 24 h under vacuum.

General Procedure for the Suzuki–Miyaura Cross-Coupling Reaction. Aryl boronic acid (0.255 mmol) and aryl halide (0.25 mmol) were taken in a 50 mL round-bottomed flask and dissolved in 2 mL of EtOH–H₂O (1:1) as the solvent. To this reaction mixture, a 2 mL ethanolic dispersion of the 5 wt % Pd–Ag@CQD nanohybrid (wrt aryl boronic acid) was added, followed by the addition of K₂CO₃ (1.0 mmol). The reactants were stirred under room temperature, and the progress of the reaction was monitored by thin-layer chromatography. After completion of the reaction, the catalyst was separated from the reaction mixture by centrifugation at 5000 rpm, washed five times with ethanol–water, and dried under vacuum. The crude reaction mixture was extracted with ethyl acetate (10 mL × 3), dried over anhydrous Na₂SO₄, followed by drying under reduced pressure. Isolation of the desired product was achieved by column chromatography using hexane and ethyl acetate as the eluent. The products were identified by ¹H and ¹³C NMR spectroscopic analyses as provided in the Supporting Information.

■ ASSOCIATED CONTENT

Supporting Information

The Supporting Information is available free of charge on the ACS Publications website at DOI: 10.1021/acsomega.7b01504.

Preparation of CQDs, images displaying the formation of the Pd–Ag@CQD nanohybrid, N₂ adsorption–desorption isotherm, table of synthesis of the Pd–Ag@CQD nanohybrid under different conditions, table of catalyst reusability screening for the Pd–Ag@CQD-catalyzed Suzuki–Miyaura coupling reaction, calculation of the mol ratio of Pd and Ag in the nanohybrid, leaching experiment of Pd and Ag, calculation of TON and TOF of the catalyst, hot filtration test for heterogeneity of the catalyst, NMR spectral analysis data (PDF)

■ AUTHOR INFORMATION

Corresponding Author

*E-mail: karakniranjan@gmail.com. Phone: +91-3712-267009. Fax: +91-3712-267006 (N.K.).

ORCID

Niranjan Karak: 0000-0002-3402-9536

Author Contributions

R.B. and N.K. contributed equally and approved the final version of the manuscript.

Notes

The authors declare no competing financial interest.

■ ACKNOWLEDGMENTS

The authors are grateful to Manali Dutta, Anurag Dutta, and Rakhee Saikia for their kind assistance during the substrate study. The authors acknowledge SAIF, NEHU, Shillong, India, for TEM analysis, CIF, IIT Guwahati and SAIC, Tezpur University, Assam, India, for various analytical support.

■ REFERENCES

- (1) Corey, E. J.; Cheng, X. M. *The Logic of Chemical Synthesis*; John Wiley & Sons: New York, 1989; pp 436–437.
- (2) Hiyama, T.; Shirakawa, E. Overview of Other Palladium-Catalyzed Cross-Coupling Protocols. In *Handbook of Organopalladium Chemistry*

for Organic Synthesis; Negishi, E. I., De Meijere, A., Eds.; John Wiley & Sons, Inc., Wiley-VCH: Weinheim, 2002; pp 285–309.

- (3) Magano, J.; Dunetz, J. R. Large-scale applications of transition metal-catalyzed couplings for the synthesis of pharmaceuticals. *Chem. Rev.* **2011**, *111*, 2177–2250.

- (4) (a) Suzuki, K.; Hori, Y.; Nishikawa, T.; Kobayashi, T. A novel (2,2-diarylviny)phosphine/palladium catalyst for effective aromatic amination. *Adv. Synth. Catal.* **2007**, *349*, 2089–2091. (b) Martin, R.; Buchwald, S. L. Palladium-catalyzed Suzuki–Miyaura cross-coupling reactions employing dialkylbiaryl phosphine ligands. *Acc. Chem. Res.* **2008**, *41*, 1461–1473. (c) Grasa, G. A.; Hillier, A. C.; Nolan, S. P. Convenient and Efficient Suzuki–Miyaura Cross-Coupling Catalyzed by a Palladium/Diazabutadiene System. *Org. Lett.* **2001**, *3*, 1077–1080. (d) Cívicos, J. F.; Alonso, D. A.; Nájera, C. Oxime palladacycle-catalyzed Suzuki–Miyaura alkenylation of aryl, heteroaryl, benzyl, and allyl chlorides under microwave irradiation conditions. *Adv. Synth. Catal.* **2011**, *353*, 1683–1687. (e) Zhou, C.; Wang, J.; Li, L.; Wang, R.; Hong, M. A palladium chelating complex of ionic water-soluble nitrogen-containing ligand: the efficient precatalyst for Suzuki–Miyaura reaction in water. *Green Chem.* **2011**, *13*, 2100–2106.

- (5) Hagen, J. *Industrial Catalysis: A Practical Approach*, 3rd ed.; Wiley-VCH: Weinheim, 2006; pp 1–5.

- (6) (a) Welch, C. J.; Albaneze-Walker, J.; Leonard, W. R.; Biba, M.; DaSilva, J.; Henderson, D.; Laing, B.; Mathre, D. J.; Spencer, S.; Bu, X.; Wang, T. Adsorbent screening for metal impurity removal in pharmaceutical process research. *Org. Process Res. Dev.* **2005**, *9*, 198–205. (b) Balanta, A.; Godard, C.; Claver, C. Pd nanoparticles for C–C coupling reactions. *Chem. Soc. Rev.* **2011**, *40*, 4973–4985. and references therein

- (7) Philippot, K.; Serp, P. Concept in nanocatalysis. In *Nanomaterials in Catalysis*; Serp, P., Philippot, K., Eds.; Wiley-VCH Verlag: Weinheim, 2013; Chapter 1, pp 1–12.

- (8) (a) Rai, R. K.; Tyagi, D.; Gupta, K.; Singh, S. K. Activated nanostructured bimetallic catalysts for C–C coupling reactions: recent progress. *Catal. Sci. Technol.* **2016**, *6*, 3341–3361. (b) Bej, A.; Ghosh, K.; Sarkar, A.; Knight, D. W. Palladium nanoparticles in the catalysis of coupling reactions. *RSC Adv.* **2016**, *6*, 11446–11453.

- (9) (a) Puthiaraj, P.; Ahn, W.-S. Highly active palladium nanoparticles immobilized on NH₂-MIL-125 as efficient and recyclable catalysts for Suzuki–Miyaura cross coupling reaction. *Catal. Commun.* **2015**, *65*, 91–95. (b) Gholinejad, M.; Seyedhamzeh, M.; Razeghi, M.; Najera, C.; Kompany-Zareh, M. Iron oxide nanoparticles modified with carbon quantum nanodots for the stabilization of palladium nanoparticles: an efficient catalyst for the Suzuki reaction in aqueous media under mild conditions. *ChemCatChem* **2016**, *8*, 441–447. (c) Gholinejad, M.; Bahrami, M.; Nájera, C. A fluorescence active catalytic support comprising carbon quantum dots and magnesium oxide doping for stabilization of palladium nanoparticles: Application as a recoverable catalyst for Suzuki reaction in water. *Mol. Catal.* **2017**, *433*, 12–19. (d) Lebaschi, S.; Hekmati, M.; Veisi, H. Green synthesis of palladium nanoparticles mediated by black tea leaves (*Camellia sinensis*) extract: Catalytic activity in the reduction of 4-nitrophenol and Suzuki–Miyaura coupling reaction under ligand-free conditions. *J. Colloid Interface Sci.* **2017**, *485*, 223–231.

- (10) (a) Sakurai, H.; Tsukuda, T.; Hirao, T. Pd/C as a reusable catalyst for the coupling reaction of halophenols and arylboronic acids in aqueous media. *J. Org. Chem.* **2002**, *67*, 2721–2722. (b) Zhao, F.; Bhanage, B. M.; Shirai, M.; Arai, M. Heck reactions of iodobenzene and methyl acrylate with conventional supported palladium catalysts in the presence of organic and/or inorganic bases without ligands. *Chem.—Eur. J.* **2000**, *6*, 843–848. (c) García-Suárez, E. J.; Lara, P.; García, A. B.; Ojeda, M.; Luque, R.; Philippot, K. Efficient and recyclable carbon-supported Pd nanocatalysts for the Suzuki–Miyaura reaction in aqueous-based media: Microwave vs conventional heating. *Appl. Catal., A* **2013**, *468*, 59–67.

- (11) (a) Chen, X.; Hou, Y.; Wang, H.; Cao, Y.; He, J. Facile deposition of Pd nanoparticles on carbon nanotube microparticles and their catalytic activity for Suzuki coupling reactions. *J. Phys. Chem. C* **2008**, *112*, 8172–8176. (b) Yang, F.; Chi, C.; Dong, S.; Wang, C.; Jia, X.; Ren,

L.; Zhang, Y.; Zhang, L.; Li, Y. Pd/PdO nanoparticles supported on carbon nanotubes: A highly effective catalyst for promoting Suzuki reaction in water. *Catal. Today* **2015**, *256*, 186–192.

(12) (a) Moussa, S.; Siamaki, A. R.; Gupton, B. F.; El-Shall, M. S. Pd-partially reduced graphene oxide catalysts (Pd/PRGO): Laser synthesis of Pd nanoparticles supported on PRGO nanosheets for carbon–carbon cross coupling reactions. *ACS Catal.* **2011**, *2*, 145–154. (b) Kakaei, K.; Dorraji, M. One-pot synthesis of Palladium Silver nanoparticles decorated reduced graphene oxide and their application for ethanol oxidation in alkaline media. *Electrochim. Acta* **2014**, *143*, 207–215. (c) Hu, J.; Wang, Y.; Han, M.; Zhou, Y.; Jiang, X.; Sun, P. A facile preparation of palladium nanoparticles supported on magnetite/s-graphene and their catalytic application in Suzuki–Miyaura reaction. *Catal. Sci. Technol.* **2012**, *2*, 2332–2340.

(13) Biffis, A.; Zecca, M.; Basato, M. Metallic palladium in the heck reaction: active catalyst or convenient precursor? *Eur. J. Inorg. Chem.* **2001**, 1131–1133.

(14) (a) Bedford, R. B.; Singh, U. G.; Walton, R. I.; Williams, R. T.; Davis, S. A. Nanoparticulate Palladium Supported by Covalently Modified Silicas: Synthesis, Characterization, and Application as Catalysts for the Suzuki Coupling of Aryl Halides. *Chem. Mater.* **2005**, *17*, 701–707. (b) Jana, S.; Dutta, B.; Bera, R.; Koner, S. Immobilization of palladium in mesoporous silica matrix: preparation, characterization, and its catalytic efficacy in carbon–carbon coupling reactions. *Inorg. Chem.* **2008**, *47*, 5512–5520.

(15) (a) Djakovitch, L.; Koehler, K. Heterogeneously catalysed Heck reaction using palladium modified zeolites. *J. Mol. Catal. A: Chem.* **1999**, *142*, 275–284. (b) Djakovitch, L.; Koehler, K. Heck reaction catalyzed by Pd-modified zeolites. *J. Am. Chem. Soc.* **2001**, *123*, 5990–5999.

(16) (a) Ramchandani, R. K.; Vinod, M. P.; Wakharkar, R. D.; Choudhary, V. R.; Sudalai, A. Pd–Cu–exchanged montmorillonite K10 clay: an efficient and reusable heterogeneous catalyst for vinylation of aryl halides. *Chem. Commun.* **1997**, 2071–2072. (b) Borah, B. J.; Borah, S. J.; Saikia, K.; Dutta, D. K. Efficient Suzuki–Miyaura coupling reaction in water: Stabilized Pdo-Montmorillonite clay composites catalyzed reaction. *Appl. Catal., A* **2014**, *469*, 350–356.

(17) (a) Zhou, S.; Johnson, M.; Veinot, J. G. C. Iron/iron oxide nanoparticles: a versatile support for catalytic metals and their application in Suzuki–Miyaura cross-coupling reactions. *Chem. Commun.* **2010**, *46*, 2411–2413. (b) Elazab, H. A.; Siamaki, A. R.; Moussa, S.; Gupton, B. F.; El-Shall, M. S. Highly efficient and magnetically recyclable graphene-supported Pd/Fe₃O₄ nanoparticle catalysts for Suzuki and Heck cross-coupling reactions. *Appl. Catal., A* **2015**, *491*, 58–69.

(18) Singh, A. S.; Patil, U. B.; Nagarkar, J. M. Palladium supported on zinc ferrite: A highly active, magnetically separable catalyst for ligand free Suzuki and Heck coupling. *Catal. Commun.* **2013**, *35*, 11–16.

(19) (a) Borah, R. K.; Saikia, H. J.; Mahanta, A.; Das, V. K.; Bora, U.; Thakur, A. J. Biosynthesis of poly(ethylene glycol)-supported palladium nanoparticles using Colocasia esculenta leaf extract and their catalytic activity for Suzuki–Miyaura cross-coupling reactions. *RSC Adv.* **2015**, *5*, 72453–72457. (b) Mahanta, A.; Mondal, M.; Thakur, A. J.; Bora, U. An improved Suzuki–Miyaura cross-coupling reaction with the aid of in situ generated PdNPs: evidence for enhancing effect with biphasic system. *Tetrahedron Lett.* **2016**, *57*, 3091–3095.

(20) Lim, S. Y.; Shen, W.; Gao, Z. Carbon quantum dots and their applications. *Chem. Soc. Rev.* **2015**, *44*, 362–381.

(21) Wang, Y.; Hu, A. Carbon quantum dots: synthesis, properties and applications. *J. Mater. Chem. C* **2014**, *2*, 6921–6939.

(22) (a) Gogoi, S.; Karak, N. Solar-driven hydrogen peroxide production using polymer-supported carbon dots as heterogeneous catalyst. *Nano-Micro Lett.* **2017**, *9*, 40. (b) Das, V. K.; Gogoi, S.; Choudary, B. M.; Karak, N. A promising catalyst for exclusive para hydroxylation of substituted aromatic hydrocarbons under UV light. *Green Chem.* **2017**, *19*, 4278.

(23) (a) Dey, D.; Bhattacharya, T.; Majumdar, B.; Mandani, S.; Sharma, B.; Sarma, T. K. Carbon dot reduced palladium nanoparticles as active catalysts for carbon–carbon bond formation. *Dalton Trans.* **2013**, *42*, 13821–13825. (b) Gholinejad, M.; Najera, C.; Hamed, F.;

Seyedhamzeh, M.; Bahrami, M.; Kompany-Zareh, M. Green synthesis of carbon quantum dots from vanillin for modification of magnetite nanoparticles and formation of palladium nanoparticles: Efficient catalyst for Suzuki reaction. *Tetrahedron* **2017**, *73*, 5585–5592.

(24) Tang, L.; Ji, R.; Cao, X.; Lin, J.; Jiang, H.; Li, X.; Teng, K. S.; Luk, C. M.; Zeng, S.; Hao, J.; Lau, S. P. Deep ultraviolet photoluminescence of water-soluble self-passivated graphene quantum dots. *ACS Nano* **2012**, *6*, 5102–5110.

(25) Shen, L.; Chen, M.; Hu, L.; Chen, X.; Wang, J. Growth and stabilization of silver nanoparticles on carbon dots and sensing application. *Langmuir* **2013**, *29*, 16135–16140.

(26) (a) Wang, X.; Cao, L.; Lu, F.; Meziani, M. J.; Li, H.; Qi, G.; Zhou, B.; Harruff, B. A.; Kermarrec, F.; Sun, Y.-P. Photoinduced electron transfers with carbon dots. *Chem. Commun.* **2009**, 3774–3776. (b) Xu, J.; Sahu, S.; Cao, L.; Anilkumar, P.; Tackett, K. N.; Qian, H.; Bunker, C. E.; Gulians, E. A.; Parenzan, A.; Sun, Y.-P. Carbon nanoparticles as chromophores for photon harvesting and photoconversion. *Chem-PhysChem* **2011**, *12*, 3604–3608.

(27) (a) De, B.; Voit, B.; Karak, N. Carbon dot reduced Cu₂O nanohybrid/hyperbranched epoxy nanocomposite: mechanical, thermal and photocatalytic activity. *RSC Adv.* **2014**, *4*, 58453–58459. (b) Duarah, R.; Singh, Y. P.; Gupta, P.; Mandal, B. B.; Karak, N. High performance bio-based hyperbranched polyurethane/carbon dot-silver nanocomposite: a rapid self-expandable stent. *Biofabrication* **2016**, *8*, 045013.

(28) Nadagouda, M. N.; Varma, R. S. Green synthesis of silver and palladium nanoparticles at room temperature using coffee and tea extract. *Green Chem.* **2008**, *10*, 859–862.

(29) Li, L.; Chen, M.; Huang, G.; Yang, N.; Zhang, L.; Wang, H.; Liu, Y.; Wang, W.; Gao, J. A green method to prepare Pd–Ag nanoparticles supported on reduced graphene oxide and their electrochemical catalysis of methanol and ethanol oxidation. *J. Power Sources* **2014**, *263*, 13–21.

(30) Verma, P.; Kuwahara, Y.; Mori, K.; Yamashita, H. Synthesis and characterization of a Pd/Ag bimetallic nanocatalyst on SBA-15 mesoporous silica as a plasmonic catalyst. *J. Mater. Chem. A* **2015**, *3*, 18889–18897.